ADVANCED MATERIALS

Surface Chemistry with the Scanning Tunneling Microscope

Surface Imaging
Surface Spectroscopy
Surface Modification
Nanolithography

By Jürgen P. Rabe*

1. Introduction

The Scanning Tunneling Microscope (STM) is a new tool in surface science, which allows for a variety of very local investigations on a preselected area of the sample. Its essential feature is a fine tip which is brought into close proximity to the sample (gap ≤ 1 nm) and whose position normal as well as parallel to the surface is controlled very accurately on an atomic length scale, i.e. ≤ 0.1 nm. The particularly precise control of the normal coordinate is accomplished by the accurate measurement of the gap width by means of the electron tunneling current between tip and sample. With this original concept[1,2] semiconductor surfaces have been imaged in ultra high vacuum (UHV) with unprecedented resolution,[3-5] local work function images have been obtained,[6] and soon it was realized that one can also get important local electron spectroscopic information with the STM,[5,7-10] including, e.g., the superconducting energy gap.[11,12]

The requirements for a sample to be investigated are sufficient electrical conductivity, sufficient flatness, and limited mobility of surface atoms or molecules. There is no requirement for any degree of order, rendering the method applicable to the study of individual defects or, e.g., metallic glasses.[13] Important for the general applicability of STM to materials science and surface chemistry is the fact that the method itself does not require UHV. Indeed, atomic resolution images have been obtained in fluid environments such as cryogenic liquids,[14,15] air,[16] water[17] and electrolytes.[18] Also solvents, oils and even greases have been used.[19,20] The only condition is that neither the electrical conductivity nor the viscosity of the fluid is too large. The advantages of the fluid environment include protection of air sensitive materials like GaAs, increased stability of the tunneling gap and a higher experimentally accessible tip voltage range.[19] Moreover, surfaces can be imaged under chemically active solutions such as electroplating solutions[18] or etchants.[21]

The STM can, however, not only be used for the characterization of surfaces but with the same instrument one can also manipulate surfaces on a scale as small as subnanometers.[22-24] Of possible technological relevance in this context is nanolithography with the STM[25-27] and, possibly, even the ability to write and read information into and from single molecules.

Other types of imaging based on related concepts have also been introduced, having in common that a fine tip is scanned across the surface and some strongly distance dependent interaction is measured while scanning. Examples of these "Scanning Tip Microscopies" are Surface Potentiometry,[28,29] Atomic Force Microscopy[30] and Scanning Thermal Profilometry,[31] the latter two being also applicable to nonconducting surfaces. However, these methods will not be discussed here any further.

While most of the early STM work was performed on clean semiconductor surfaces in UHV, this field will only be briefly mentioned here. The interested reader is referred to other reviews[32-34] and the proceedings of the three International Conferences on Scanning Tunneling Microscopy.[35-37] Also the application of STM to nonconducting samples, either coated with an ultrathin conducting film[38-40] or replicated[41] will not be discussed in detail here. This review will, however, cover surface chemistry, imaging of organic molecules at surfaces and surface modifications with the STM.

2. The Method

Electron tunneling is a common phenomenon on the atomic scale, which allows electrons to penetrate into classically forbidden regions in space. The probability of finding an electron at increasing distances away from a nucleus decreases exponentially outside an atom. If one brings an atomically sharp metallic tip close (≤ 1 nm) to an electrically conducting surface a tunneling current will flow when a small potential difference (of the order of 1 V or less) is applied between the two. To a first approximation, the current depends exponentially on the gap width, decreasing by about one order of magnitude for every Ångstrom of increase in gap spacing. It is this very high sensitivity to the gap width which makes the tunneling current a suitable signal to control the gap by means of a feedback loop. The accuracy can be better than 0.01 nm.

If the tip is now scanned across the surface while the current is sensed, a topograph of the surface can be obtained in two ways. In the constant current mode[1,2] the tip height is adjusted with the feedback loop maintaining a constant current. The image is obtained as a map of the tip height $z(x, y)$ versus the lateral coordinates x and y (Fig. 1). Alternatively, in the constant height mode[42] the tip is

[*] Dr. J. P. Rabe
Max-Planck-Institut für Polymerforschung
Postfach 3148, D-6500 Mainz (FRG)

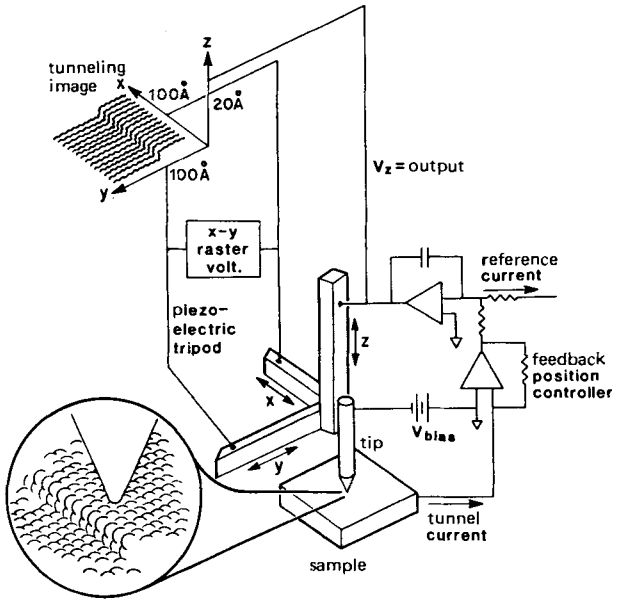

Fig. 1. Schematic illustration of the Scanning Tunneling Microscope [32]. The tunnel current from tip to sample, induced by V_{bias}, is maintained constant by an electronic feedback system (right), which controls the tip position normal to the sample surface via the z-leg of the piezoelectric tripod. A record of the z-leg feedback voltage, as the x-y tripod legs raster scan the tip laterally, constitutes a tunneling image, which is a form of replica of the sample surface (inset at bottom).

scanned at constant height and the current I (x, y) is recorded as a function of x and y. In the latter case the limiting frequency of the feedback loop must be smaller than the frequency of current variations due to atomic structure. The feedback loop serves only to maintain the average current constant.

Common to all the published instrument designs are piezoelectric elements as x-, y- and z-translators. After the initially devised tripod[1,2] the simpler single tube[43] arrangement became widely used as a compact and fast scanner. Sample positioning, originally achieved with a piezoelectric walker ("louse")[1,2] has been simplified by differential springs, levers[44] or, elegantly, with a piezoelectric translator relying on the moment of inertia.[45] While external vibration isolation was essential in the earlier instruments, newer designs are often so small and rigid that it became less important or even obsolete.[46] Also the operating temperature range has been increased to extend from 4.2 K to 350 K.[11,46]

An essential feature of the STM is the tip. Different materials have been used, including W, Pt/Ir, Au and carbon. Also, tips have been prepared according to different procedures, e.g. mechanically ground or electrochemically etched. For use under liquid, they have been coated with glass or polymer, leaving only the last few microns bare. However, it appears that many results are fairly independent of the particular tip preparation recipe. On the other hand, since the formation of the outermost cluster of atoms on a macroscopic tip is usually not well controlled, some variation in instrumental resolution is observed even with equal tip preparation. Also the tip may change during scanning. In an attempt to obtain tips controlled to an atomic level, they have been reproducibly prepared and subsequently characterized in a field ion microscope.[47]

A theory of the STM[48,49] has been developed, based on the transfer Hamiltonian of *Bardeen*.[50] Assuming an ideal tunneling geometry (tip on flat) the tunneling current was found to be proportional to the local density of states (LDOS) of the surface at the center of curvature of the tip and at the Fermi energy. In the constant current mode the STM image then represents simply a contour of constant LDOS. In the usual case of an extended Fermi surface the image gives basically the contour of constant total charge density. In an attempt to determine how the LDOS is reflected in STM images the apparent size of an adsorbed atom has been studied as a function of bias for several different atoms.[51-53]

3. Conductor Surfaces

Gold was one of the first surfaces studied with the STM.[1,2,54-57] While the early studies in UHV revealed monoatomic steps and corrugation due to surface reconstructions, later also atomic corrugation of the close packed Au (111) surface was reported in both UHV and air.[58] Furthermore, hills on evaporated gold films, typically about 2 nm high, have been observed under a number of fluids, including glycerol, silicone- and paraffin-oil as well as several greases.[20]

The hexagonal reconstruction of Pt (100) has been imaged in UHV at terraces and domain boundaries.[59,60] Silver films on mica, exhibiting (111) surfaces, can be atomically flat across terraces several tens of in diameter. Atomic resolution images in air reveal, however, not the silver lattice but a larger lattice, possibly from a semiconducting surface layer of about monolayer thickness.[61]

While aluminum in air forms too insulating an oxide for STM imaging, niobium, on the other hand, forms a surface oxide layer which is sufficiently conducting for stable tunneling. Films prepared by vapor deposition at room temperature are fairly rough, but deposition at elevated substrate temperature gives considerably smoother films.[62]

Highly oriented pyrolytic graphite (HOPG) is a semimetal, which has been imaged at atomic resolution in UHV[63] and in a variety of fluids, e.g., air,[16] water,[17] electrolytes[18] and liquid helium.[15] It forms large (diameter ≈ 1 μm) atomically perfect, flat terraces, which are chemically inert; moreover, the spatial variation of the LDOS is very pronounced, resulting in high contrast images with a resolution of about 0.2 nm. However, attempts to use HOPG as a well characterized substrate to image monomolecular adsorbates on it with the STM suffered from its excessive inertness. In this context, defects may be of importance and have therefore been investigated in some de-

ADVANCED MATERIALS

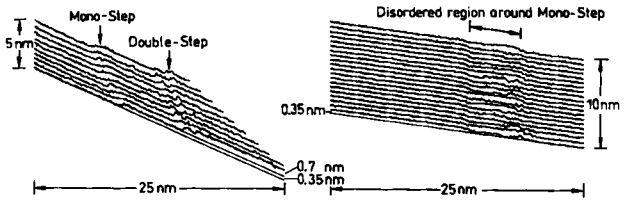

Fig. 2. STM images of mono- and bilayer steps on graphite in the constant current mode [64].

tail[64] (Fig. 2 and 3). Amorphous carbon, on the other hand, forms very flat films with grain sizes of the order of some nanometers[40,65] The problem of adhesion of adsorbates (e.g. a polymer) to graphite is also of interest in carbon fiber composites technology. Interestingly, carbon fiber surfaces can be imaged with the STM at atomic resolution.[64]

The first atomic resolution STM images were obtained on a silicon (111) surface in UHV with its 7×7 reconstruction ,[3] and it was also this surface which gave early electron spectroscopic results.[5,8-10] Experiments on freshly prepared silicon surfaces in air are, however, only possible for a limited time due to the formation of an insulating oxide surface layer.[66] In an attempt to avoid the oxide formation under ambient conditions a chemical preparation is required, which terminates dangling silicon bonds. For hydrogen terminated silicon atomically flat surfaces have been observed.[67] Other semiconductor surfaces investigated in detail include GaAs (110)[68] and, e.g., several lov index faces of the group IV semiconductors Si, Ge anc Sn.[69]

While direct local electron spectroscopic studies witl the STM proved very successful in UHV, they appear more difficult in air or under liquids. Nevertheless, there also i is the electronic surface structure which is sensitively probed. An example of this is charge density waves in TaS_2. While STM images of native TaS_2 are dominated by a charge density wave state,[14,70] titanium doping systematically perturbs this electronic feature so that the surface structure can be imaged directly (Fig. 4).[71,72] It is expected that systematic studies of chemically modified surfaces will also lead to a better understanding of STM images.

Generally speaking, it appears easier to obtain atomic resolution images of semimetals or semiconductors than of simple metals. This has been attributed to the smeared-out electronic wavefunction in the case of metals

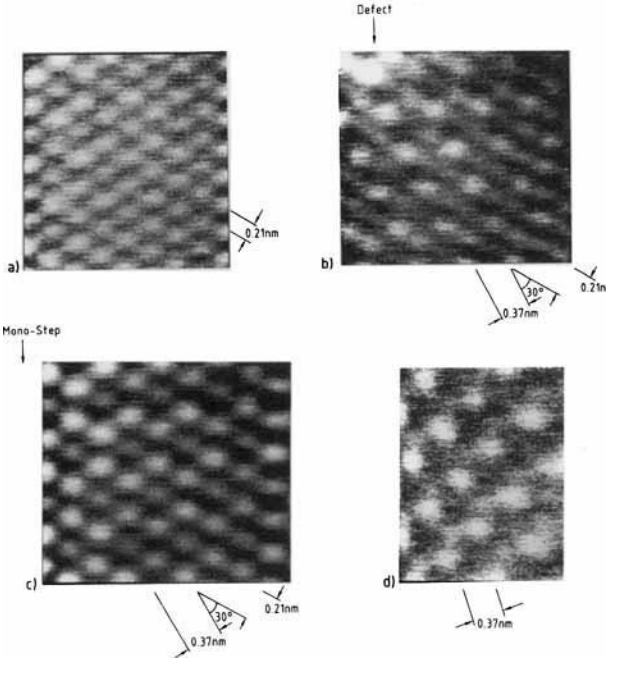

Fig. 3. STM images in the constant height mode [64]. a) Highly oriented pyrolytic graphite (HOPG). b) $\sqrt{3} \times \sqrt{3}$ R 30° superstructure near localized defect on graphite. c) Inverse $\sqrt{3} \times \sqrt{3}$ R 30° structure next to graphite step. d) $\sqrt{3} \times \sqrt{3}$ R 30° structure dominating STM image close to a defect. Intensity of superstructure relative to graphite image decays away from the defect over some 3 nm.

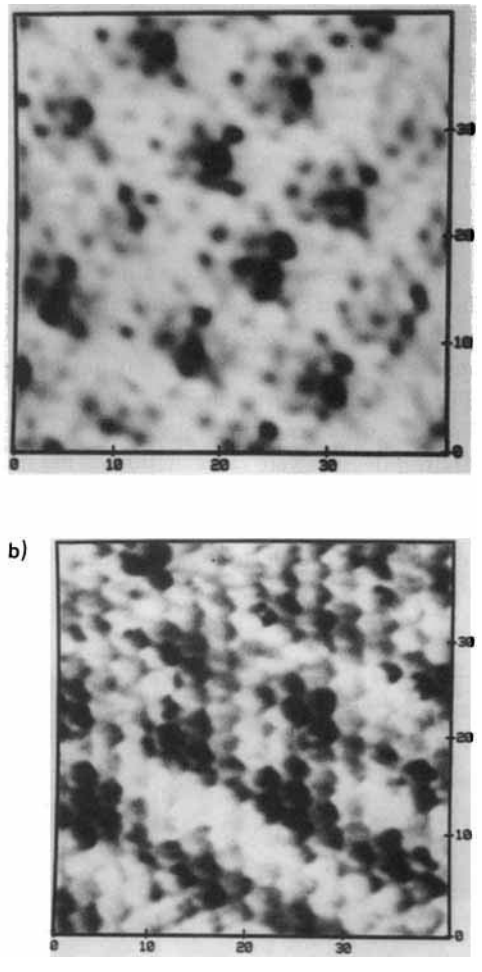

Fig. 4. Gray scale image of $Ti_xTa_{1-x}S_2$ recorded in the constant current mode [72]. The sample surfaces were covered with oil to improve the image stability. a) $x = 0.06$; The gray scale in this image (black minimum to white maximum) is 0.43 nm. b) $x = 0.1$; The gray scale in this image, 0.29 nm, is significantly smaller than in (a). The tip bias voltages are +8 mV and +9 mV, respectively, the tunneling current is 2.1 nA. x- and y-axes markings are in 0.1 nm.

and the large spatial variation of the LDOS of semiconductors, where higher contrast, higher resolution images and also more detailed spectroscopic information are obtained. In fact, the fairly high contrast in the atomic resolution images of the noble metals is difficult to interpret. Clearly, semiconductor surface studies in UHV have to date made by far the largest contribution of STM to high resolution microscopy and spectroscopy, partly since STM is well suited for these studies and partly since these surfaces had already been extensively investigated by other techniques.

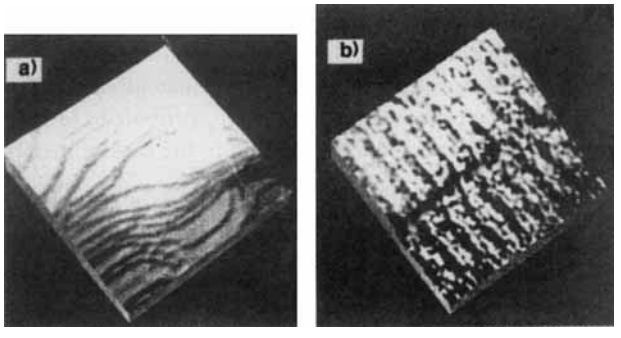

Fig. 5. STM images of the TTF-TCNQ surface [73]. a) A 200×200 nm^2 area. The surface is terraced, with steps approximately 1 nm high. b) A 10×10 nm^2 area in which rows of molecules are seen at a step.

The first molecularly resolved image of an organic conductor has been obtained on tetrathiafulvalene tetracyanoquinodimethane (TTF-TCNQ) crystals,[73] revealing monomolecular steps and the unit cell on the crystal surface (Fig. 5). Also some features in the STM image could be reproduced by simulations in which contours of constant electron density were calculated from the molecular orbitals that are involved in conduction (Fig. 6). These results suggest that the STM will also be a useful tool for the investigation of the electronic properties of organic conductors.

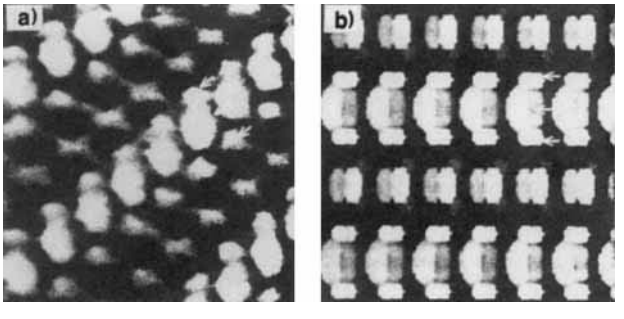

Fig. 6. Comparison of an experimental STM image and a theoretical simulation of the TTF-TCNQ surface [73]. a) A 2.5×2.5 nm^2 scan with a total height range of 0.9 nm. Lighter regions are higher. Arrows indicate a row of triplets of balls assigned to individual TCNQ molecules. b) A 2.5×2.5 nm^2 simulated image. Arrows indicate a row of TCNQ molecules along the *b* direction.

4. Organic Adsorbates

For an adsorbate to be imaged with the STM it is necessary that 1) the underlying substrate is sufficiently flat, 2) molecular mobility is not too high, and 3) the current through the molecule is sufficient. A number of atomically flat substrates such as graphite, suitably prepared gold and silver or silicon are available. However, the fact that some of these substrates can be imaged at atomic resolution in a variety of fluid environments indicates that in these cases the mobility of the environments adsorbates is too high for them to appear on the images in any way other than noise. On the other hand, adsorbates bonded chemically to a surface can be imaged. Moreover, their interaction with the substrate can be studied by imaging the electronic structure of the substrate close to the adsorbate. An example is the band bending around oxygen adsorbed on GaAs (110),[74] which reaches as far as 5 nm away from the adsorbate. Another example is a defect such as an adsorbate on graphite, which results in a superlattice appearing superimposed on the STM image of graphite and decaying away from the defect.[64, 75]

Clear examples of atom resolved surface chemistry are the imaging of chemical bond formation after adsorption of NH_3 on Si (001)[76] and a mapping of the reactivity of dangling bond states on Si (111)-(7×7).[77] For NH_3 as an adsorbate it was found that Si rest atoms are more reactive than Si adatoms and that center adatoms are more reactive than corner adatoms. Probing dangling bond states on both clean and NH_3-exposed surfaces revealed interactions and charge transfer between sites, influencing surface reactivity (Fig. 7).[77]

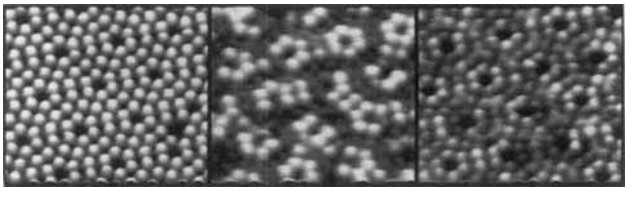

Fig. 7. Topographs [77] of the unoccupied states of a) a clean Si (111)-(7×7) surface (tip voltage = 0.8 V), b) partially reacted surface (tip voltage = 0.8 V), and c) partially reacted surface (tip voltage = 3.0 V).

Highly resolved images of organic adsorbates have been obtained on an ordered (3×3) superlattice of coadsorbed benzene and carbon monoxide on a rhodium (111) surface (Fig. 8).[78] While images on the close packed monolayer are very stable, for submonolayer coverage diffusion increases and it is observed that an individual molecule changes places during the STM scan of one image.

A similar situation is encountered for phthalocyanines on copper (100). While it appeared difficult to image a single phthalocyanine molecule on silver,[79] regular arrays of these molecules on Cu (100) could be observed and under

ADVANCED MATERIALS

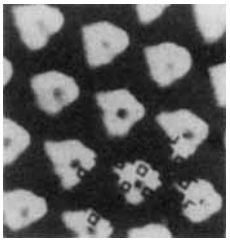

Fig. 8. STM image of an ordered (3 × 3) superlattice of coadsorbed benzene and carbon monoxide on rhodium (111) [78]. At tip voltage <0.5 V a nominally threefold structure with a depression in the center is observed. According to the superimposed mesh based on the LEED model, the lobes appear to be localized between, rather than over, the underlying metal atoms.

some circumstances atomic scale features were observed, which agree well with Hückel molecular orbital calculations.[80] Attempts to image multilayers gave neither regular structures nor very high resolution, indicating that in this case the conductivity of the layer may be too small to allow for a nondestructive observation.

Studies on larger organic molecules have also been reported, including a whole single virus,[81] fatty acid salts,[82] lipid/protein membranes,[83] DNA,[84] several synthetic polymers such as phthalocyaninato-polysiloxane[64], poly-octadecylmethacrylate and poly-methylmethacrylate[85] and a liquid crystalline material,[86] all on graphite.

However, the interpretation of these experiments is difficult, since the tunneling distances are rather large and also the intrinsic conductivities often appear too small to explain the current densities used in the experiments. Here there may be significant surface conductivity due to adsorbed water and salts, which are always present in biological preparations. As a matter of fact, molecularly resolved images of macroscopically thick paraffin have been reported to be of varying quality, depending on the ambient humidity.[84] Another issue is the notoriously poor adhesion of adsorbates to graphite. While it may be enhanced around defects in the substrate, it is necessary to distinguish those defects carefully from an adsorbate.[64] It appears that this has not always been done. The interpretation is further complicated if one takes into account a deformation of the molecule during scanning.[87] In conclusion, while apparently several polymers have been imaged with the STM, clearly more work is necessary to understand the situation as well as in the case of the inorganic conductors.

5. Surface Modification with the STM

The STM setup also provides a means of modifying surfaces on an atomic scale and imaging the effect immediately afterwards. This is achieved by raising the tip voltage for a short time (e.g. 100 ns) to a value of the order of 4 V. However, the processes involved are not fully understood. For a germanium surface it was suggested that a transfer of tip material to the sample may occur.[22] For graphite immersed in an organic liquid (phthalates) it was argued that individual organic molecules had become selectively attached to the substrate.[23] On the other hand it was observed that similar modifications could be obtained without these specific molecules (Fig. 9).[24] For metallic glasses it has been suggested that local melting is responsible.[88] Though lithography on a nanometer scale has been shown to be possible,[25-27] more understanding is necessary to control the modifications better. This includes their dimensions as well as their stability, which, e.g. due to diffusion, can be limited to a time scale of hours.[24, 89]

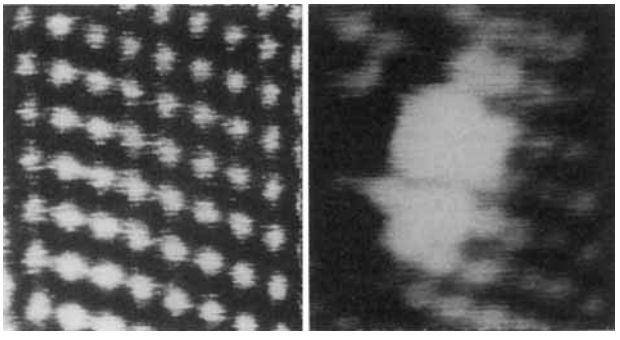

Fig. 9. STM images of highly oriented pyrolytic graphite (HOPG) in air in the constant height mode [24]. Tip voltage 100 mV, tunneling current 2 nA. Left: Atomic resolution image, representing for a flat terrace of about 1 μm diameter, before applying a voltage pulse. Right: Same area after applying a 100 ns pulse of 3.5 V. The surface has been modified on an area of about $0.5 \times 1.0\ nm^2$.

6. Outlook

The STM is not only a microscope, local electron spectrometer and lithographer, it quite generally provides very locally injected low energy electrons for analytical or manipulative purposes. For example, the tunneling electrons can cause local excitations which then may decay radiatively. The corresponding light can be analyzed spectroscopically, leading to an optical spectroscopy with molecular spatial resolution.[90] Indeed, the STM appears to be close to what *R. P. Feynman* had asked for in 1960:[91] A machine, capable of storing and reading information on a small scale, say 100 atoms. Today it is envisioned that the miniaturization of computing may lead to a molecular electronics: single molecules acting as diodes, switches or molecular wires. Here the STM may provide the means to address the particular molecule.

Received: November 7, 1988

[1] G. Binnig, H. Rohrer, *Helv. Phys. Acta 55* (1982) 726.
[2] G. Binnig, H. Rohrer, C. Gerber, E. Weibel, *Phys. Rev. Lett. 49* (1982) 57.
[3] G. Binnig, H. Rohrer, C. Gerber, E. Weibel, *Phys. Rev. Lett. 50* (1983) 120.
[4] R. S. Becker, J. A. Golovchenko, E. G. McRae, B. S. Swartzentruber, *Phys. Rev. Lett. 55* (1985) 2028.

[5] R. M. Tromp, R. J. Hamers, J. E. Demuth, *Phys. Rev. B34* (1986) 1388.
[6] G. Binnig, H. Rohrer, *Surf. Sci. 126* (1983) 236.
[7] G. Binnig, K. H. Frank, H. Fuchs, N. Garcia, B. Reihl, H. Rohrer, F. Salvan, A. R. Williams, *Phys. Rev. Lett. 55* (1985) 991.
[8] R. S. Becker, J. A. Golovchenko, D. R. Hamann, B. S. Swartzentruber, *Phys. Rev. Lett. 55* (1985) 2032.
[9] R. S. Becker, J. A. Golovchenko, B. S. Swartzentruber, *Phys. Rev. Lett. 55* (1985) 987.
[10] R. J. Hamers, R. M. Tromp, J. E. Demuth, *Phys. Rev. Lett. 56* (1986) 1972.
[11] S. A. Elrod, A. L. de Lozanne, C. F. Quate, *Appl. Phys. Lett. 45* (1984) 1240.
[12] A. L. Lozanne, S. A. Elrod, C. F. Quate, *Phys. Rev. Lett. 54* (1985) 2433.
[13] R. Wiesendanger, M. Ringger, L. Rosenthaler, H. R. Hidber, P. Oelhafen, H. Rudin, H. J. Güntherodt, *Surf. Sci. 181* (1987) 46.
[14] R. V. Coleman, B. Drake, P. K. Hansma, C. G. Slough, *Phys. Rev. Lett. 55* (1985) 394.
[15] D. P. E. Smith, G. Binnig, *Rev. Sci. Instrum. 57* (1986) 2630.
[16] S. Park, C. F. Quate, *Appl. Phys. Lett. 48* (1986) 112.
[17] R. Sonnenfeld, P. K. Hansma, *Science (Washington) 232* (1986) 211.
[18] R. Sonnenfeld, B. C. Schardt, *Appl. Phys. Lett. 49* (1986) 1172.
[19] J. Schneir, P. K. Hansma, *Langmuir 3* (1987) 1025.
[20] B. Giambattista, W. W. McNairy, C. G. Slough, A. Johnson, L. D. Bell, R. V. Coleman, J. Schneir, R. Sonnenfeld, B. Drake, P. K. Hansma, *Proc. Natl. Acad. Sci. USA 84* (1987) 4671.
[21] R. Sonnenfeld, J. Schneir, B. Drake, P. K. Hansma, D. E. Aspnes, *Appl. Phys. Lett. 50* (1987) 1742.
[22] R. S. Becker, J. A. Golovchenko, B. S. Swartzentruber, *Nature (London) 235* (1987) 419.
[23] J. S. Foster, J. E. Frommer, P. C. Arnett, *Nature (London) 331* (1988) 324.
[24] J. P. Rabe, unpublished.
[25] M. Ringger, H. R. Hidber, R. Schlögl, P. Oelhafen, H. J. Güntherodt, *Appl. Phys. Lett. 46* (1985) 832.
[26] M. A. McCord, R. F. W. Pease, *J. Vac. Sci. Technol. B4* (1986) 86.
[27] M. A. McCord, R. F. W. Pease, *J. Vac. Sci. Technol. B6* (1988) 293.
[28] P. Muralt, D. W. Pohl, *Appl. Phys. Lett. 48* (1986) 514.
[29] J. R. Kirtley, S. Washburn, M. J. Brady, *Phys. Rev. Lett. 60* (1988) 1456.
[30] G. Binnig, C. F. Quate, C. Gerber, *Phys. Rev. Lett. 56* (1986) 930.
[31] C. C. Williams, H. K. Wickramsinghe, *Appl. Phys. Lett. 49* (1987) 1587.
[32] J. A. Golovchenko, *Science (Washington) 232* (1986) 48.
[33] G. Binnig, H. Rohrer, *Angew. Chem. 99* (1987) 622; *Angew. Chem. Int. Ed. Engl. 26* (1987) 606.
[34] P. K. Hansma, J. Tersoff, *J. Appl. Phys. 61* (1987) R1.
[35] Proc. 1st Int. Conf. Scanning Tunneling Microscopy, *Surf. Sci. 181* (1987).
[36] Proc. 2nd Int. Conf. Scanning Tunneling Microscopy, *J. Vac. Sci. Technol. A6* (1988) 257.
[37] Proc. 3rd Int. Conf. Scanning Tunneling Microscopy, *J. Microsc. (Oxford)*, in press.
[38] R. C. Jaklevic, L. Elie, W. Shen, J. T. Chen, *J. Vac. Sci. Technol. A6* (1988) 488.
[39] M. Amrein, A. Stasiak, H. Gross, E. Stoll, G. Travaglini, *Science (Washington) 240* (1988) 514.
[40] R. Guckenberger, C. Kösslinger, R. Gatz, H. Breu, N. Levai, W. Baumeister, *Ultramicroscopy 25* (1988) 111.
[41] J. A. N. Zasadzinski, J. Schneir, J. Gurley, V. Elings, P. K. Hansma, *Science (Washington) 239* (1988) 1013.
[42] A. Bryant, D. P. E. Smith, C. F. Quate, *Appl. Phys. Lett. 48* (1986) 832.
[43] G. Binnig, D. P. E. Smith, *Rev. Sci. Instrum. 57* (1986) 1688.
[44] J. E. Demuth, R. J. Hamers, R. M. Tromp, M. E. Welland, *J. Vac. Sci. Technol. A4* (1986) 1320.
[45] K. Besocke, *Surf. Sci. 181* (1987) 145.
[46] J. W. Lyding, S. Skala, J. S. Hubacek, R. Brockenbrough, G. Gammie, *Rev. Sci. Instrum.*, in press.
[47] H.-W. Fink, *IBM J. Res. Dev. 30* (1986) 460.
[48] J. Tersoff, D. R. Hamann, *Phys. Rev. Lett. 50* (1983) 1998.
[49] J. Tersoff, D. R. Hamann, *Phys. Rev. B31* (1985) 805.
[50] J. Bardeen, *Phys. Rev. Lett. 6* (1961) 57.
[51] N. D. Lang, *Phys. Rev. Lett. 56* (1986) 1164.
[52] N. D. Lang, *Phys. Rev. B34* (1986) 5947.
[53] N. D. Lang, *Phys. Rev. Lett. 58* (1987) 45.
[54] G. Binnig, H. Rohrer, C. Gerber, E. Weibel, *Surf. Sci. 131* (1983) L379.
[55] G. Binnig, H. Rohrer, C. Gerber, E. Stoll, *Surf. Sci. 144* (1984) 321.
[56] W. J. Kaiser, R. C. Jaklevic, *Surf. Sci. 181* (1987) 55.
[57] W. J. Kaiser, R. C. Jaklevic, *Surf. Sci. 182* (1987) L227.
[58] V. M. Hallmark, S. Chiang, J. F. Rabolt, J. D. Swalen, R. J. Wilson, *Phys. Rev. Lett. 59* (1987) 2879.
[59] R. J. Behm, W. Hoesler, E. Ritter, G. Binnig, *Phys. Rev. Lett. 56* (1986) 228.
[60] E. Ritter, R. J. Behm, G. Potsche, J. Wintterlin, *Surf. Sci. 181* (1987) 403.
[61] J. P. Rabe, H. Fuchs, unpublished.
[62] D. G. Walmsley, R. J. Turner, H. P. Hagan, N. Garcia, A. Baró, L. Vazquez, R. Paganini, *J. Vac. Sci. Technol. A6* (1988) 404.
[63] G. Binnig, H. Fuchs, C. Gerber, H. Rohrer, E. Stoll, E. Tosatti, *Europhys. Lett. 1* (1986) 31.
[64] J. P. Rabe, M. Sano, D. Batchelder, A. A. Kalatchev, *J. Microsc. (Oxford) 152* (1988) in press.
[65] A. Stemmer, A. Engel, R. Häring, R. Reichelt, U. Aebi, *Ultramicroscopy 25* (1988) 171.
[66] K. H. Besocke, M. Teske, J. Frohn, *J. Vac. Sci. Technol. A6* (1988) 408.
[67] W. J. Kaiser, L. D. Bell, M. H. Hecht, F. J. Grunthaner, *J. Vac. Sci. Technol. A6* (1988) 519.
[68] R. M. Feenstra, J. A. Stroscio, J. Tersoff, A. P. Fein, *Phys. Rev. Lett. 58* (1987) 1192.
[69] R. S. Becker, B. S. Swartzentruber, J. S. Vickers, *J. Vac. Sci. Technol. A6* (1988) 472.
[70] C. G. Slough, W. W. McNairy, R. V. Coleman, B. Drake, P. K. Hansma, *Phys. Rev. B34* (1986) 994.
[71] X.-L. Wu, C. M. Lieber, *J. Am. Chem. Soc. 110* (1988) 5200.
[72] X.-L. Wu, P. Zhou, C. M. Lieber, *Nature (London) 335* (1988) 55.
[73] T. Sleator, R. Tycko, *Phys. Rev. Lett. 60* (1988) 1418.
[74] J. A. Stroscio, R. M. Feenstra, A. P. Fein, *Phys. Rev. Lett. 58* (1987) 1668.
[75] H. Mizes, J. S. Foster, unpublished.
[76] R. J. Hamers, Ph. Avouris, F. Boszo, *Phys. Rev. Lett. 59* (1987) 2071.
[77] R. Wolkow, Ph. Avouris, *Phys. Rev. Lett. 60* (1988) 1049.
[78] H. Ohtani, R. J. Wilson, S. Chiang, C. M. Mate, *Phys. Rev. Lett. 60* (1988) 2398.
[79] J. K. Gimzewski, E. Stoll, R. R. Schlittler, *Surf. Sci. 181* (1987) 267.
[80] P. H. Lippel, R. J. Wilson, M. D. Miller, Ch. Wöll, S. Chiang, unpublished.
[81] A. M. Baró, R. Miranda, J. Alaman, N. Garcia, G. Binnig, H. Rohrer, C. Gerber, J. L. Carrascosa, *Nature (London) 315* (1985) 253.
[82] D. P. E. Smith, A. Bryant, C. F. Quate, J. P. Rabe, C. Gerber, J. D. Swalen, *Proc. Natl. Acad. Sci. USA 84* (1987) 969.
[83] J. K. H. Hörber, C. A. Lang, T. W. Hänsch, W. M. Heckl, M. Möhwald, *Chem. Phys. Lett. 145* (1988) 151.
[84] M. Amrein, G. Travaglini, R. Dürr, A. Stasiak, H. Gross, H. Rohrer, *3rd Int. Conf. Scanning Tunneling Microscopy*, Oxford 1988.
[85] T. R. Albrecht, M. M. Dovek, C. A. Lang, P. Grütter, C. F. Quate, S. W. J. Kuan, C. W. Frank, R. F. W. Pease, *J. Appl. Phys. 64* (1988) 1178.
[86] J. S. Foster, J. E. Frommer, *Nature (London) 333* (1988) 542.
[87] S. M. Lindsay, T. Thundat, L. A. Nagahara, *J. Microsc. (Oxford)*, in press.
[88] U. Staufer, R. Wiesendanger, L. Eng, L. Rosenthaler, H.-R. Hidber, H.-J. Güntherodt, *J. Vac. Sci. Technol. A6* (1988) 537.
[89] J. Schneir, O. Marti, G. Remmers, D. Gläser, R. Sonnenfeld, B. Drake, P. K. Hansma, *J. Vac. Sci. Technol. A6* (1988) 283.
[90] J. H. Coombs, J. K. Gimzewski, B. Reihl, J. K. Sass, R. R. Schlittler, *J. Microsc. (Oxford)*, in press.
[91] R. P. Feynman, *Engin. Sci. 1960*, February issue, p. 22.